

# InfraRed Search & Track Systems as an Anti-Stealth Approach

George-Konstantinos Gaitanakis<sup>1</sup>, Andreas Vlastaras<sup>2</sup>, Nikolaos Vassos<sup>3</sup>, George Limnaios<sup>4</sup> and Konstantinos C. Zikidis<sup>5</sup>

## Abstract

For more than half a century, the radar has been indisputably the most important sensor in the battlefield, especially in the air domain. Radars have always been competing with electronic warfare systems, which are trying to hinder detection and tracking with the use of various jamming techniques. However, the apparition of stealth or low observable technology since the late '80s has been the game changer which has really contested the radar dominance. Therefore, other parts of the electromagnetic spectrum have been revisited, in an effort to substitute or complement the radar. In this way, infrared seems to be a viable approach. Even if significant efforts have been exerted in order to minimise the IR signature of fighter aircraft, it is impossible to make a fast flying jet, propelled by hot exhaust gases, completely disappear, in the IR spectrum. InfraRed Search & Track orIRST systems offer significant advantages with respect to traditional radar systems, such as passive operation, resistance to jamming, and long detection ranges (under certain conditions). On the other hand, there is no direct range measurement, as in the radar case. This paper begins with a brief presentation of various military applications of IR, followed by an update on currentIRST systems. An approach to the estimation of the detection distance of a jet fighter by anIRST system is then proposed. This approach is based on the modelling of a typical turbofan engine and of a modernIRST system. In the simulation, various weather conditions and different fields of view are taken into account. It is shown that, under favourable conditions, the detection range of a non-afterburning engine, observed from behind, is at the order of 100 km or more, outperforming the typical fighter radar in terms of detection against stealth threats.

**Keywords:** InfraRed Search & Track (IRST), Planck's law, MODTRAN, Beer's law, effective aperture, field of view, transmittance, spectral detectability.

## 1 Introduction

---

<sup>1</sup> Hellenic Army Academy, Vari, Attika, Greece. e-mail: [gaitanakisgiwrgos@yahoo.gr](mailto:gaitanakisgiwrgos@yahoo.gr)

<sup>2</sup> 3, 4, 5 Hellenic Air Force Academy, Dekelia Air Base, Greece. e-mail: [kzikidis@cs.ntua.gr](mailto:kzikidis@cs.ntua.gr)

Infrared radiation (IR) is invisible electromagnetic radiation, with longer wavelengths than red light, typically covering the spectrum from 300 GHz (wavelength 1 mm or 1000  $\mu\text{m}$ ) up to 430 THz (0.7  $\mu\text{m}$ ). Every object with a temperature above absolute zero emits electromagnetic radiation, mainly in the IR band. Objects at higher temperatures emit also visible light, as in the case of the incandescent light bulb. The spectral density of electromagnetic radiation emitted by a black body in thermal equilibrium is given by Planck's law [1].

As IR travels through the atmosphere, it is absorbed by water vapour, carbon dioxide, carbon monoxide, nitrous oxide, etc., leaving only certain "windows" (the sub-bands of 3-5 and 8-12  $\mu\text{m}$ ) allowing for decent propagation. In Fig. 1 is depicted the transmittance of atmosphere over 1 nautical mile at sea level [2]. Transmittance generally improves with altitude.

Concerning the case of an aircraft, it exhibits a complex thermal signature, emanating from the following components:

- Engine "hot parts" (aft turbine face, engine centre, body and interior nozzle surface).
- Engine exhaust plumes (emissions from the fuel combustion, mainly carbon dioxide and water vapour).
- Airframe, which includes all of the external surfaces of the wings, fuselage, canopy etc., as well as solar and terrestrial reflections and Mach shock wave (aerodynamic heating).

Therefore, any vehicle flying into the air unavoidably emits thermal radiation, which can be detected, if it exhibits sufficient contrast against the cold background.

The most common device exploiting this feature against an air target is the heat-seeking missile, which has a history of more than half a century. Apart from IR homing,IRST systems have been used since the late '50s for detection and targeting purposes, in the air-to-air domain. Being passive sensors,IRST systems provide serious advantages, since they do not alert the adversary. Furthermore, they cannot be jammed as easily as the radar. They also offer much better angular resolution with respect to the radar but they cannot measure distance directly.

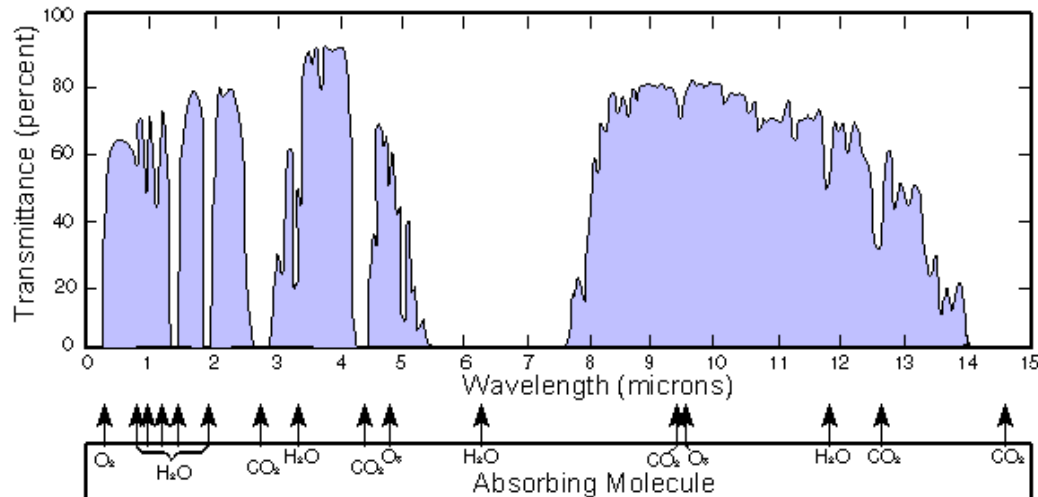


Figure 1: IR Transmittance of atmosphere at sea level over 1 nautical mile [2]. Most useful “windows” are mid-wave IR (MWIR) with wavelength 3-5  $\mu\text{m}$  and long wave IR (LWIR) with wavelength 8-12  $\mu\text{m}$ .

In the modern air-naval-land warfare, in addition to fighter aircraft,IRST technology is employed in maritime air defence systems, as well as in battle tank Active Protection Systems (APS). With the development of data fusion in modern combat systems, significant improvements in effectiveness can be achieved with the combination, association and correlation of data from multiple sensors and sources, such as the radar andIRST system (range – angular precision) [3].

On the other hand, IR systems are more sensitive than radar to adverse weather conditions. Therefore, taking into account the advances in radar technology,IRST systems were abandoned in the U.S. 15-20 years ago, with the venerable F-14D Tomcat being the lastIRST-equipped fighter.

Stealth aircraft, apart from their Radar Cross Section (RCS) reduction, employ techniques reducing their IR signature, as well. Such techniques are the omission of an afterburner (as in the case of the F-117 and B-2), the use of high bypass ratio turbofan engines (where the bypass stream is used to cool the exhaust gases), and the placement of the exhaust duct on the top, in an effort to hide the hot gases from below (as in the case of B-2). Some aircraft use their fuel as coolant, transferring waste heat to it, e.g., the F-35. Despite all these efforts, it is simply impossible to make such a

heat source, as a fast flying aircraft, disappear in the IR band. Therefore,IRST systems appear to be a viable anti-stealth approach.

Contrary to the U.S., the Russians have never given up onIRST, equipping most of their fighters since the '60s with such systems. The Chinese, who are advancing fast on stealth design, equip their Chengdu J-20 and Shenyang FC-31 with advanced electro-optical systems, which appear to be similar in concept to the ones of the F-35. Furthermore, during the last decades, all modern European fighters (Rafale, Eurofighter Typhoon, Gripen NG, which are unofficially referred to as "euro-canards") are featuring latest generationIRST systems, with advanced capabilities. Following these advances, which may put the U.S. stealth advantage into peril, Americans have recently re-discoveredIRST systems, trying to catch up with Europe and Russia.

In the following section, IR military applications and currentIRST systems are presented. In the 3<sup>rd</sup> section, a mathematical model of a modernIRST is presented, in order to predict the detection range of a turbofan engine model, under various weather conditions and fields of view. The simulation yields plausible results, indicating exceptional performance under certain conditions.

## **2 Historical Background and Current Trends**

As mentioned above, one of the first military applications exploiting the IR band was the heat-seeking missile. The most notable example is the AIM-9 Sidewinder. Development began right after the 2<sup>nd</sup> World War, in 1946. Ten years later, the AIM-9A/B had entered production. Initially used by the U.S. Navy, it outperformed its USAF counterpart, the AIM-4 Falcon, and eventually equipped USAF fighters as well. Initial versions (up to AIM-9J) used a PbS detector in the Short-Wave IR band (1.9-2.6  $\mu\text{m}$ ), while following versions (from AIM-9L to AIM-9P) were equipped with an InSb one (4 $\mu\text{m}$ , MWIR), permitting "all aspect" engagements (attack from all directions, not only from the rear quarter).

With each new version, there were improvements regarding mainly missile range and guidance system, where more advanced detector technology allowed longer detection ranges, while was also efficiently rejecting Infrared Counter Measures (IRCM), such as flares. The latest version is the AIM-9X Block II, employing a

MWIR focal plane array seeker. The AIM-9X, apart from air-to-air, can be also used in surface-to-air applications. Other air-to-air missiles of the heat seeker family are the British ASRAAM, the IRIS-T stemming from a German-led multinational program, the French MICA IR (a medium range missile, with data link, dual-band seeker and thrust vectoring), and the Russian R-73. Modern seekers employ two separate sensors, using also a LWIR sensor (apart from the MWIR), in order to discriminate the target from flares or other decoys, making use of HgCdTe (Mercury Cadmium Telluride) cells.

A similar family of missiles are the Man-portable air-defence systems (MANPADS), which are mainly shoulder-launched surface-to-air missiles against low flying targets (up to 10.000 ft), such as helicopters. Most of these missiles employ infrared homing, with guidance systems similar to the air-to-air missiles described above, including focal plane array for the latest generation. Examples of this category are the U.S. Stinger (later versions of which make use also of UV radiation), the French Mistral, and the Russian systems Iгла and Strela. The maximum range of these missiles is in the class of 4 nautical miles.

Another family in the IR electro-optics are the Forward Looking IR or FLIR systems. These are more complex thermal imaging cameras, exploiting MWIR, mainly for air-to-ground. They provide infrared image used for navigation, surveillance, recognition, and targeting purposes, during day or night. Examples of systems containing a FLIR subsystem are the LANTIRN navigation and targeting pod system (AN/AAQ-13 and -14, respectively), the AN/AAQ-33 Sniper Advanced Targeting Pod, the AN/ASQ-228 Advanced Targeting FLIR (ATFLIR), the AN/AAQ-28(V) LITENING targeting pod, the Damocles targeting pod, as well as the "Target Acquisition and Designation Sights, Pilot Night Vision System" (TADS/PNVS) of the AH-64 Apache helicopter. Most of the above systems are also equipped with visible-light HDTV, laser rangefinder and laser target designator subsystems, for targeting purposes. Many helicopters are equipped with FLIR systems, in order to perform surveillance at all times.

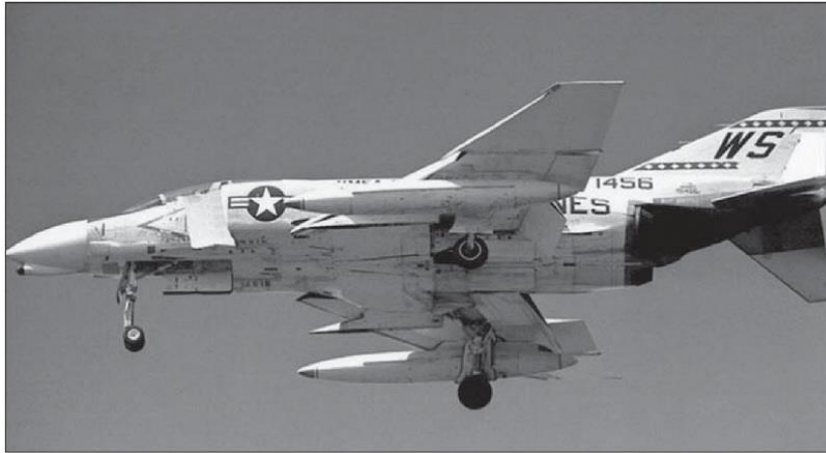


Figure 2: A Phantom F-4B featuring the AAA-4 infrared seeker head, mounted beneath the radar. Due to improvements in the AIM-9 Sidewinder and low utilisation, this seeker was not retained in later F-4 versions [4].

InfraRed Search & Track (IRST) systems are non-imaging devices exploiting initially LWIR and later LWIR or MWIR, for air-to-air detection and targeting purposes. The first IRST systems appeared in the late '50s – early '60s, on U.S. interceptors, such as the F-101 Voodoo, F-102 Delta Dagger, and F-106 Delta Dart. They were also used on the F-8E Crusader, the F-4 Phantom (see Figure 2), and the Swedish J-35A and J-35F-2 Draken. These were simple infrared seekers, performing horizontal scanning and slaved to a display under the main radar display. Any IR signal falling on the sensor would create a blip on the display, allowing the pilot to manually turn the radar to the relevant angle, trying to detect the target by the radar. These primitive systems were of limited utility and were abandoned when more advanced radar systems appeared.



Figure 3: A U.S. Navy F-14D Super Tomcat preparing to connect with a tanker with its refuelling probe out. One can observe under the chin, the AN/AXX-1 Television Camera Set (TCS) and the AN/AAS-42 IRST (with the dark dome). Retired in 2006, this had been until recently the last IRST-equipped U.S. fighter.

In the '90s, the AN/AAS-42 IRST was developed, which was a more advanced sensor, with a LWIR scanned linear array (even though initially there was a MWIR, as well), employed on the Tomcat F-14D (also called Super Tomcat). It was placed under the radar, operating in six discrete modes similar to the AN/APG-71 radar. According to Jane's, a 3-axis inertially stabilised gimbal allows the system to accurately search multiple scan volumes, either automatically or under manual pilot control. This was a quite capable IRST sensor, “designed to permit the multiple tracking of thermal energy emitting targets at extremely long ranges to augment information supplied by conventional tactical radars”. Newer versions of this sensor, were subsequently fitted to export fighters, such as the F-15SG Eagle ordered by Singapore, as part of the “TIGER Eyes” sensor suite.

However, the F-14D was retired from the USN in 2006. At that time, the USAF seemed rather reluctant to adopt such a sensor, deciding not to fund the development of AIRST (Advanced IRST), which was intended to equip the F-22 Raptor. Taking into account that there was no equivalent sensor in the U.S. inventory, this left the U.S. without an IRST-equipped fighter for some time.

This trend is changing and the U.S. seem to be rediscovering the IRST:

- The F-35 is equipped with two electro-optical systems, the AN/AAQ-37

Distributed Aperture System (DAS) and the AN/AAQ-40 Electro-Optical Targeting System (EOTS). DAS is a dual-band system (MWIR and LWIR), comprising 6 IR sensors around the aircraft for full spherical coverage, providing day/night imaging and acting as an IRST and missile approach warning system. EOTS combines FLIR and IRST functionality, mainly for air-to-ground purposes, sharing many modules with the Sniper Advanced Targeting Pod, although it is fitted internally. An “Advanced EOTS” has been proposed to replace EOTS in newer F-35 blocks, featuring various enhancements, including short-wave infrared (SWIR).

- In 2015, the USN approved the low-rate initial production of the IRST21 sensor system, in order to equip the F/A-18 Super Hornet with IRST. The IRST21 sensor is based on the legacy AN/AAS-42 IRST and is mounted in the nose of the F/A-18E/F’s centreline fuel tank. The IRST21 is also the main sensor of the Legion Pod, a multi-function sensor system which supports collaborative targeting operations. In 2017, the Legion Pod was selected for the U.S. F-15C.
- At the same time, the OpenPod IRST was presented, as a future solution providing targeting, communications, LIDAR and further options. The OpenPod is an evolution of the LITENING pod, with the integration of IRST technology developed in Europe for the PIRATE and SkyWard.



Figure 4: An F-16 equipped with the Legion Pod sensor system. Integration and flight tests have been completed on F-16 (image from the manufacturer's website).

Concerning Europe, all modern European jet fighters feature advanced IRST systems, as follows (in order of appearance):

- The French Rafale employs the OSF (Optronique Secteur Frontal or Front Sector Optronics – FSO), which comprises dual band IRST/FLIR, TV and Laser rangefinder, for air-to-air and air-to-ground surveillance and targeting. It was the first dual band IR system (MWIR and LWIR) in the West. However, at the current standard of Rafale (F3) the OSF retains only the TV/Laser subsystem, since the IR subsystem is considered obsolete, and will be replaced by an upgraded one at the future standard F4.
- The Eurofighter Typhoon employs the EuroFirst Passive InfraRed Airborne Track Equipment (PIRATE), a dual-band IRST/FLIR system, able to detect and track air and surface targets and provide FLIR imagery for low level flight and navigation during all-weather, day or night operations. It is stated to perform also passive ranging.
- The JAS 39E/F Gripen NG features the SkyWard which is based on the experience gained from the Eurofighter Typhoon's PIRATE. This system uses a LWIR focal plane array sensor (with dual band capability as a potential upgrade) and is stated to be “capable of detecting low-RCS targets at distances compatible with a beyond-visual-range missile launch”. The SkyWard is claimed to exhibit anti-stealth capabilities, since “*some infrared absorbent paints cause more friction than standard surfaces, and that causes kinetic heating that the IRST will pick up*”, according to manufacturer's officials [5]. It can also perform “kinetic ranging”, where the carrier aircraft performs a specific manoeuvre and the range is determined by the change in azimuth angle to the target. The range can be estimated with the help of another Gripen via triangulation, with data exchanged over the TAU-Link (Tactical Air Unit data link).



Figure 5: The 101KS-V IRST of the Sukhoi Su-57 (previously T-50 or PAK-FA) can be seen in front of the canopy, starboard side (image from the UAC website).

Regarding Russia, they have been equipping their fighters, such as the MiG-23, the Su-27, and the MiG-31, with IRST since the '60s. IRST systems have always been present on Russian fighters, as a countermeasure against the more advanced radars of the western fighters. In this way, Russian fighters would acquire an enemy aircraft at reasonable ranges, without the enemy aircraft being warned. Current Russian IRST systems are the OLS-27/30/35 for the Flanker family and the OLS-29 for their Mig-29/35 counterparts. Also, the 101KS-V (OLS-50M) is an advanced IRST being developed as part of the 101KS Atoll Electro-Optical system for the Su-57 5<sup>th</sup> gen. fighter. The 101KS-V IRST is reported to be based on Quantum Well Imaging Photodetector (QWIP) technology, operating in a much wider spectral bandwidth that includes the very long-wave 15  $\mu\text{m}$  band to detect very cool targets.

China is catching up fast on the 5<sup>th</sup> gen. fighter domain, developing the Chengdu J-20 and the Shenyang FC-31, in a way similar to the F-22 & F-35 hi-lo mix. The EOTS-89 electro-optical targeting system and the EORD-31 IRST are under development for J-20 and J-31. Marketing brochures list detection ranges for the B-2 at 150km and for the F-22 up to 110km. Both J-20 and FC-31 are reported to feature also a distributed aperture system similar to DAS of the F-35.

### 3 Modelling the engine, the weather, and the IRST sensor

Taking into consideration the above, the following questions arise: which is the maximum range a stealth fighter aircraft would be detected by an IRST sensor? Furthermore, which are the most important parameters affecting this range?

Trying to answer these questions, the following steps were followed:

- Modelling of the target aircraft engine, based on characteristics of a typical turbofan engine, such as the F135, the powerplant of the F-35.
- Analysis of the weather conditions and atmosphere transmittance, using the MODTRAN model.
- Analysis of the IRST sensor, i.e., detector, optics, etc., using characteristics and parameters pertaining to the PIRATE or the SkyWard systems.
- Estimation of maximum detection distance based on the radiant intensity difference between target and background.

The turbofan is the most common jet engine type today, offering more thrust and less fuel consumption with respect to older turbojet engines, at usual flight regimes (high subsonic – low supersonic speeds). There are various analyses on turbofan engine operation, e.g., [6] [7]. The bypass ratio, i.e., the ratio of the air mass-flow bypassing the engine core to the air mass-flow passing through the core, for a fighter aircraft turbofan is less than 1:1, e.g., 0.36:1 for the Pratt & Whitney F100, powering the F-16 and the F-15, or 0.57:1 for the F135-PW-100 of the F-35A CTOL (Conventional Take Off and Landing). Fighter aircraft use engines with low bypass ratios, as a compromise between fuel economy and combat requirements, such as high power-to-weight ratio, supersonic performance, and the ability to use afterburner. Moreover, the bypass air flow cools the exhaust plume, reducing the overall IR signature of the aircraft.

However, the temperature of the exhaust plume is not very important at long ranges, because its main components, carbon dioxide and water vapour, play a significant role in IR absorption. In other words, the radiation of the plume is emitted at discrete frequencies, which are strongly attenuated as the distance between the target and the IRST increases [8]. It is estimated that less than 5% of the incident radiation of the plume on the IRST detector contributes to target detection, at long

distances. On the other hand, the exhaust plume is the main source of radiation for heat seeking missiles, because at short distances the emitted radiation has not been attenuated yet. For example, detectors of MANPADS or air-to-air missiles have the optimum performance at the wavelength of  $4.35\mu\text{m}$ , which corresponds to the radiation emitted by carbon dioxide [8].

In the proposed approach, the last stage of the turbine and the inner surface of the exhaust duct are considered as the main sources of radiation. The engine is supposed to be on military thrust (without the use of the afterburner). Concerning the F-35, the area of the nozzle of the F135 engine is estimated at  $0.32\text{-}0.72\text{ m}^2$ . For the simulation, the aperture of the nozzle is considered to be  $0.51\text{ m}^2$

### 3.1 Beer's law

According to Beer's law (or Beer-Lambert law):

$$t = e^{-\alpha R} \quad (1)$$

where  $t$  is the transmittance,  $\alpha$  is the weather coefficient model, depending on the weather conditions prevailing at the area, and  $R$  is the range of the target from the sensor. Apart from the weather conditions, the coefficient depends on the atmospheric window where the sensor exhibits maximum efficiency. In the simulation, a MWIR IRST is considered, operating in the atmospheric window  $3\text{-}5\ \mu\text{m}$ . As far as the atmospheric conditions are concerned, the following cases are considered:

- drought conditions ( $\alpha = 0.05$ ),
- clean atmosphere ( $\alpha = 0.1$ ),
- light dust or haze ( $\alpha = 0.4$ ),
- rainfall ( $\alpha = 0.8$ ),
- high intensity rainfall ( $\alpha = 1.2$ ).

### 3.2 The sky radiation

The sky radiation is an important factor for the simulation, taking into account that it reaches also the sensor, reducing the contrast between the target and the background. The MODTRAN (MODerate resolution atmospheric TRANsmission) condition model was used in order to simulate the weather condition model. MODTRAN software computes line-of-sight (LOS) atmospheric spectral transmittances and radiances. The following parameters were used:

- Mid-Latitude Winter
- Altitude: 10 Km (a little more than 30 kft)
- 90° degrees zenith angle
- visibility: 10Km
- aerosol mode: rural

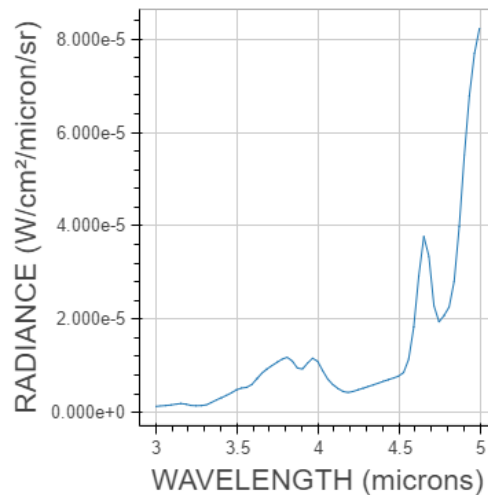


Figure 6 : In the above diagram, which results from the MODTRAN model, one can consider as value of sky radiation:  $E=2 \cdot 10^5$  W/cm<sup>2</sup>/micron/sr. This is a conservative approach, given that in the window of 3-4.6  $\mu\text{m}$  the sky radiation is smaller than this value.

### 3.3 System requirements

Following an approach similar to the radar detection of signals in noise, there are certain requirements concerning performance for an IRST. More specifically, the probability of detection ( $P_d$ ) of the target should be higher than 95% and the false alarm rate ( $FAR$ ) should be lower than one per hour [10]:

$$P_d = 0.95 \quad (2)$$

$$FAR = 0.0001 \quad (3)$$

From the diagram of probability of detection for given values of  $FAR$  (e.g., fig. 4.160 of [10]), one can find the required  $SNR$  (Signal to Noise Ratio). The  $SNR$  value that satisfies the said requirements is 5.8.

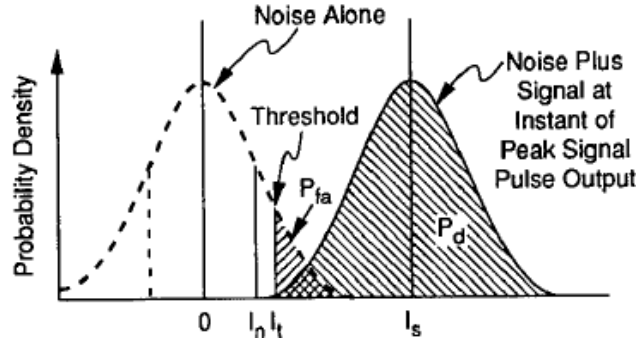


Figure 7: Detection of a target in a noisy environment [10].

### 3.4 The IRST Model

A modern IRST sensor would exhibit an array of  $640 \times 512$  detectors, while according to [11], the next generation will have an array size of  $1024 \times 1024$ . So, let's assume a standard  $640 \times 512$  array. The frames an IRST can see depend on the field of view. The following three cases of field of view were examined in the simulation, which are the ones stated for the SkyWard IRST [12]:

- Wide Field Of View (WFOV):  $30^\circ \times 24^\circ$
- Medium Field Of View (MFOV):  $16^\circ \times 12.8^\circ$
- Narrow Field Of View (NFOV):  $8^\circ \times 6.4^\circ$

The wider the field of view is, the easier to look at the direction of the target but also more sky radiation (noise) will be in the frame, reducing the contrast. On the other hand, a narrow field of view would provide a good contrast, due to less sky radiation entering the frame, allowing the detection of a target from far away, provided that the sensor is looking at the target. So, there is no perfect solution but only a compromise on this issue.

Each frame is divided to pixels, depending on the array size of the sensor. An  $640 \times 512$  sensor means that this is the number of discrete elements horizontally and vertically. As the number of pixels increases, the size of each one decreases, as well as the sky radiation entering the relevant element of detection. In the simulation, the target radiation is considered to fall into one pixel and not to a set of pixels or to any area in between. In this way, the total radiation of the target can be exploited for the purpose of detection. Therefore, a more dense array (with more pixels) means that less sky radiation will enter each pixel, including the pixel of detection.

According to [13], in a modern IRST, the pitch (the distance between the centres of adjacent pixels) is approximately  $16\mu\text{m}$ . Supposing that the size of each

pixel is approximately 15.52  $\mu\text{m}$  (97% of the pitch), the fill factor of the array is estimated at 0.94 (94%) [14], which is a realistic, albeit conservative, assumption.

### 3.5 Estimation of Detection Range

Following the reasoning of [15], the maximum distance  $R$  at which the target can be detected is estimated according to the following formula:

$$R^2 = \frac{\pi D_0 t_0 t D^*}{4F\#\sqrt{\omega\Delta f SNR}} \left[ \int_{\lambda_1}^{\lambda_2} J_t(\lambda) d\lambda - \int_{\lambda_1}^{\lambda_2} J_b(\lambda) A d\lambda \right] \quad (4)$$

Where

- $D_0$  is the effective calibre or effective aperture of the optical system. If we suppose that  $D_0$  is circular (as it usually is), then its diameter  $d_0$  is related to the focal length  $f$  and the f-number  $F\#$  of the optical system by the equation:

$$d_0 = f/F\# \quad (5)$$

In the simulation, the three following values of  $d_0$  were used, corresponding to the three different modes of field-of-view (Wide, Medium, Narrow):  $d_w = 15.16\text{mm}$ ,  $d_m = 28.4\text{mm}$ ,  $d_n = 56.8\text{mm}$ .

- $t$  is the transmittance coefficient of the atmosphere, as in eq.1 (Beer's law). It depends on the distance of the target and the weather conditions [9].

- $t_0$  is the transmittance coefficient of the optical system itself. For example, the PIRATE has 90 reflecting surfaces, containing the overall attenuation of the input radiation [16]. Therefore,  $t_0$  attenuates even further the radiation from the target. Assuming a moderate value for  $t_0$ , in the simulation runs it is set that  $t_0=0.78$ , even though better (higher) transmittance coefficients can be found in current optical systems.

- $D^*$  is the spectral detectability or specific detectivity, a performance characteristic of each detector technology. According to [18], for PIRATE, a peak value of  $D^*$  is assumed to be  $1.5 \cdot 10^{11} \text{cm} \sqrt{Hz}/W$  for MWIR. In this simulation, a  $D^*$  with a value of  $1.4 \cdot 10^{11} \text{cm} \sqrt{Hz}/W$  is assumed for the detectors. A more thorough analysis on  $D^*$  is provided in [17].

- $F\#$  is the f-number, that is the ratio of the optical system's focal length to the diameter of the detector array, as mentioned in eq. 5.  $F\#$  and the wavelength are related to the size of the diffraction-limited optical spot, as follows:

$$F\# = \frac{d}{2.44 * \lambda} \quad (6)$$

where  $d$  is the detector size and  $\lambda$  the centre wavelength. In the simulation,  $d=15.52\mu\text{m}$  and  $\lambda=4,95\mu\text{m}$ , so  $F\#$  is approximately 1.29.

- The angle  $\omega$  represents the instantaneous field of view (*IFOV*) or the angular resolution of the detector. For small values, *IFOV* is approximated by:

$$IFOV \approx \frac{d}{f} \quad (7)$$

with  $d$  the detector size and  $f$  the focal length. The above formula applied to the whole array becomes:

$$f = \frac{\text{array dimension}}{FOV} \quad (8)$$

The horizontal dimension of the array for 640 detectors with pitch  $16\mu\text{m}$  will be  $640 \times 16\mu\text{m} = 10.24\text{mm}$ . For the 512 detectors, the vertical dimension of the array will be  $512 \times 16\mu\text{m} = 8.192\text{mm}$ . So, the array dimension (diagonal) will be  $\sqrt{10.24^2 + 8.192^2}\text{mm} = 13.1136\text{mm}$ . The FOV is not stable and depends on the function mode. For example, for wide function mode (WFOV), FOV is  $30^\circ \times 24^\circ$ . So, the average angular resolution is  $\sqrt{30^2 + 24^2} = 38.41^\circ$  or  $670.38\text{mrad}$ . So, the focal length for WFOV from eq. 8 will be  $f = 13.1136\text{mm}/0.67038\text{rad}$  or  $f=19.56\text{mm}$ . According to eq. 7, *IFOV* will be  $0.7934\text{ mrad}$  or  $0.0454^\circ$ . The relevant parameters can be computed in the same way for MFOV and NFOV.

- $\Delta f$  is the equivalent bandwidth of noise of system, which can be expressed as follows [15]:

$$\Delta f = 1/2t_d \quad (9)$$

where  $t_d$  is the sampling or dwell time. For a sampling frequency of 3Hz, the dwell time is 0.3333 sec and  $\Delta f$  is 1.5 Hz.

- The *SNR* value has been estimated previously and should be equal to 5.8.

•  $J_t$  is the radiant intensity of both target and background and  $J_b$  is the radiant intensity of background, in the wave band under consideration (3-5 $\mu$ m). They are calculated as follows, starting with  $J_t$  [15]:

$$J_t = \sigma \varepsilon_t A_t T_t^4 n_{\Delta\lambda} / \pi \quad (10)$$

where:

$\sigma = 5.67032 \times 10^{-12} \text{ W} \cdot \text{cm}^{-2} \cdot \text{K}^{-4}$  is the Stefan-Boltzmann constant.

$\varepsilon_t$  is the emitting coefficient of target. In the simulation:  $\varepsilon_t = 0.90$ .

$A_t$  is the surface of the target, i.e., the F135 nozzle. In our simulation,  $A_t = 0.51 \text{ m}^2$ .

$T_t$  is the temperature of the target. The temperature of the inner engine surface is estimated at  $T_t = 1000^\circ \text{ K}$ .

$n_{\Delta\lambda}$  is the bandwidth factor and shows what percentage of the total radiance of the target is emitted within the waveband under consideration. In the simulation, it is assumed that  $n_{\Delta\lambda} = 0.31$ .

The target is considered to be a Lambertian surface, so the radiant intensity is divided by  $\pi$ .

• Concerning now the background radiant intensity  $J_b$ , we have:

$$J_b = \sigma \varepsilon_b (\omega R^2 - A_t) T_b^4 n'_{\Delta\lambda} / \pi \quad (11)$$

where:

$\sigma = 5.67032 \times 10^{-12} \text{ W} \cdot \text{cm}^{-2} \cdot \text{K}^{-4}$  is the Stefan-Boltzmann constant.

$\varepsilon_b$  is the emitting coefficient of background. In the simulation:  $\varepsilon_b = 0.90$ .

$\omega R^2$  is the surface that the IFOV covers at the moment of detection in  $\text{m}^2$ . Obviously, it depends on the distance of the target from the sensor. Moreover, IFOV changes in the three different modes of Narrow-Medium-Wide. The background radiant intensity is received from the area that the IFOV covers minus the surface of the target:

$$\omega R^2 - A_t$$

$T_b$  is the environment temperature at 30000ft. It is assumed that  $T_b = 230^{\circ}K$ , following the tables of U.S. Standard Atmosphere Heights and Temperatures.

$n'_{\Delta\lambda}$  is the bandwidth factor and shows what percentage of the total radiance of the background is emitted within the waveband under consideration. Following a similar approach as above, it is assumed that  $n'_{\Delta\lambda}=0.31$ .

## 4 Simulation results

Following [19], a metric of theIRST capability to detect a point target is the evaluation of the ratio:

$$\frac{\lambda * F\#}{d} \quad (12)$$

where  $\lambda$  is the wavelength, the  $F\#$  is the F-number, and  $d$  is the linear dimension of the detector pixel. This ratio has to be less than 0.5 for a system suited for detection. For this simulation, this ratio yields 0.41, indicating a suitable system, as far as the basic quality requirements are concerned.

Taking into account the above models and reasoning, the results for certain weather conditions and fields of view are depicted in Table 1.

Table 1: Simulation results ofIRST detection range (in km), at high altitude. The engine is on dry thrust (no afterburner) and theIRST is behind the target aircraft.

<b>Weather Conditions</b>	<b>WFOV</b> (Wide FOV)	<b>MFOV</b> (Medium FOV)	<b>NFOV</b> (Narrow FOV)
Drought	109-136.6	128-169.1	147-180.1
Clean atmosphere	70-93	79-110	88-137
Dust - haze	42.5	52	61
Rainfall	30.3	41.6	48.8
Strong rainfall - snow	12.2-20	13.9-24.5	14.8-27

From the above results, it is clear that, in good weather conditions, a target (e.g., an F-35, as in our case) can be detected at quite long distances, in the order of 100 km, or even more in drought conditions. Comparable detection distances have been reported for real systems in actual trials [20], indicating the plausibility of the proposed approach.

As the weather conditions are getting worse, the performance of theIRST deteriorates. At heavy rainfall or snow,IRST detection range becomes quite poor.

However, in most cases, IRST detection range is better than the expected detection range of a stealth jet by a typical tactical aircraft radar [21].

The field of view significantly affects performance. As FOV gets wider, the contrast between target and background is reduced and the performance is poor. On the other hand, for narrow FOV, the performance is considerably better. However, it is more difficult to use such a narrow mode for detection.

It is noted that the proposed approach takes into account only the engine hot parts, seen from behind, and not aerodynamic friction. Future work will also examine the phenomenon of aerodynamic heating of leading edges and engine inlets and the relevant effect in terms of IRST detection.

## 5 Conclusion

IRST systems provide an alternative means of detection against enemy aircraft. They offer certain advantages compared to the typical aircraft fire control radars, such as covert operation, immunity to jamming, and higher angular resolution. In certain conditions, IRST systems offer also exceptionally long detection ranges, challenging conventional radars. On the other hand, they do not measure range directly, as radars do. However, modern IRST systems employ indirect methods for range measurement, featuring passive ranging.

Developments in weapon systems, especially the appearance of stealth threats, have led to a renewal of interest in IRST systems, which now offer more advanced sensor technology and better signal processing techniques compared to the past. The United States seem to be rediscovering the IRST, trying to catch up with Europe, Russia, and China, despite the fact that they had been using IRST systems almost half a century ago.

Trying to investigate the possible operational advantage of a modern IRST system for the purpose of detecting stealth aircraft, this work examines an engine model based on the Pratt&Whitney F135 of the F-35, an IRST model based on characteristics of state-of-the-art IRST systems, and a methodology to estimate the maximum detection range. Several cases were simulated with this approach, corresponding to different weather conditions and fields of view of the sensor.

The detection ranges obtained are quite close to values reported from real IRST tests, proving the validity of the proposed approach. The results indicate that

detection range is affected by several parameters, most notably by the weather conditions and the field of view. However, in most cases, IRST performance is quite good, allowing target detection at operationally significant distances, whether this target is stealth or not. Therefore, IRST is proved to be a valuable sensor, considerably augmenting situational awareness, especially with respect to stealth threats, against which conventional tactical radars are almost useless.

## References

- [1] Max Planck, *The theory of heat radiation*, P. Blakiston's Son & Co, Philadelphia, 1914.
- [2] *Electronic Warfare and Radar Systems - Engineering Handbook*, NAWCWD TP 8347 4th Ed., Naval Air Warfare Center Weapons Division, Point Mugu, California, 2013.
- [3] G.-K. Gaitanakis, K. C. Zikidis and G. P. Kladis, Multi-sensor Data Fusion for 3D Target Tracking: A Synergy of Radar and IRST (InfraRed Search & Track), presented at the *Int'l Scientific Conference "eRA-12"*, Piraeus University of Applied Sciences (PUAS), Attica, Greece, 24-25 October 2017.
- [4] Peter E. Davies, *US Marine Corps F-4 Phantom II Units of the Vietnam War*, Osprey Publishing, Oxford, UK, 2012.
- [5] Bill Sweetman, Gripen Sensors Claim Counter-Stealth Performance, *Aviation Week & Space Technology*, Mar 17, 2014. <http://aviationweek.com/awin/gripen-sensors-claim-counter-stealth-performance>
- [6] Philip Hill and Carl Peterson, *Mechanics and Thermodynamics of Propulsion* (2nd Edition), Pearson, 1991.
- [7] Thomas W. Wild and Michael J Kroes, *Aircraft Powerplants*, 8th Edition, McGraw-Hill Education, 2013.
- [8] G.A. Rao and S.P. Mahulikar, Aircraft Powerplant and Plume Infrared Signature Modelling and Analysis, *43rd AIAA Aerospace Sciences Meeting and Exhibit*, 10 - 13 January 2005, Reno, Nevada, USA.
- [9] Björn Hässler, Atmospheric Transmission Models for Infrared Wavelengths, *Master thesis*, Linköping University, (1998).
- [10] Stephen B. Campana, ed., *Passive Electro-Optical Systems*, The Infrared and Electro-Optical Systems Handbook – Volume 5, Infrared Information Analysis

- Center, Michigan, and SPIE Optical Engineering Press, 1993.
- [11] Ian Moir and Allan Seabridge, *Military Avionics Systems*, Wiley press, 2006.
- [12] Leonardo Airborne and Space Systems, *SkyWard IRST Technical Characteristics*. <http://www.leonardocompany.com/en/-/skyward-1>
- [13] USAF Scientific Advisory Board, *New world vistas: Air and space power for the 21st century : munitions volume*, University of Michigan Library, 1996.
- [14] D. Knežević, A. Redjimi, K. Mišković, D. Vasiljević, Z. Nikolić and J. Babić, Minimum resolvable temperature difference model, simulation, measurement and analysis, *Optical and Quantum Electronics*, **48**(332), (2016).
- [15] Hanping Wu and Xinjian Yi, Operating Distance Equation and Its Equivalent Test for Infrared Search System with Full Orientation, *International Journal of Infrared and Millimeter Waves*, **24**(12), (2003), 2059–2068.
- [16] Luigi Enrico Guzzetti, Livio Busnelli, EF2000 PIRATE Test flights campaign, *Proc. of SPIE* **7109**, (2008).
- [17] Paul R . Norton, *Handbook of Optics*, Third Edition, **II**(15), (2009).
- [18] P.V. Coates, The Fusion of an IR Search and Track With Existing Sensors To Provide a Tracking System for Low Observability Targets, *AGARD*, **AG-337**, (1996), 32 - 47.
- [19] B. Sozzi, E. Fossati, G. Barani, N. Santini, A. Ondini, G. Colombi and C. Quaranta, Simulator of IRST system with ATR embedded functions, *Proc. SPIE* **7660**, *Infrared Technology and Applications XXXVI*, 766003, (2010).
- [20] Ingmar A. Andersson, Leif Haglund, SAAB IRST: the system and flight trials, *Proc. SPIE* **4820**, *Infrared Technology and Applications XXVIII*, (2003).
- [21] P. Touzopoulos, D. Boviatsis and K.C. Zikidis, 3D Modelling of Potential Targets for the purpose of Radar Cross Section (RCS) Prediction, *Proceedings of the 6th International Conference on Military Technologies (ICMT2017)*, Brno, Czech Republic, (2017), 636 – 642.